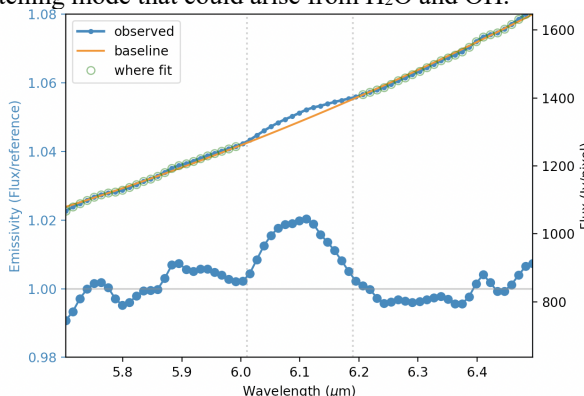


**MOLECULAR WATER IN THE LUNAR FAR SOUTH USING 6 MICRON SPECTRAL IMAGING.** W. T. Reach<sup>1</sup>, P. G. Lucey<sup>2</sup>, C. I. Honniball<sup>3</sup>, A. Arredondo<sup>4</sup>, E. R. Malaret<sup>5</sup>. <sup>1</sup>Universities Space Research Association, NASA Ames Research Center, ([wreach@usra.edu](mailto:wreach@usra.edu)), <sup>2</sup>Hawai'i Institute of Geophysics and Planetology, University of Hawai'i at Mānoa, <sup>3</sup>NASA Goddard Space Flight Center, <sup>4</sup>Southwest Research Institute, <sup>5</sup>ACT Gate.

**Introduction:** The existence of water on the Moon is now well established by observations including Chandrayaan-1 Moon Mineralogy Mapper (M3) [1], LCROSS [2], LRO UV and laser reflectance [3], and direct measurement in lunar samples, at more than the parts per million (ppm) level, significantly higher than the parts per billion that had been accepted before the 21<sup>st</sup> century [4,5]. Here, we study the southern polar region, in order to search for correlations between water and other localized surface features. Prior observations demonstrated the presence of H<sub>2</sub>O on the sunlit surface [6]. The region near the lunar south pole is of high importance for future space exploration, with multiple spacecraft preparing to go there, including the soon-to-launch VIPER mission [7].

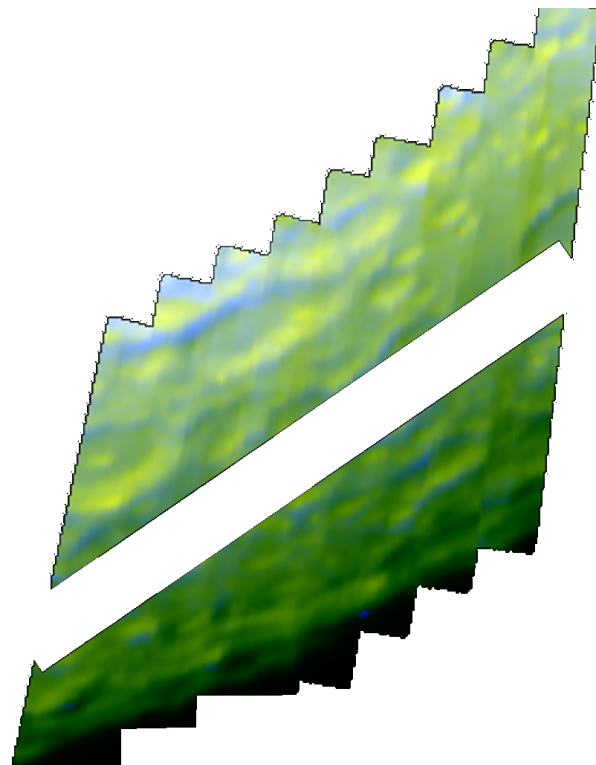
**Observations:** We used the Stratospheric Observatory for Infrared Astronomy (SOFIA) [8] on 2022 Feb 17 to measure a 6.1  $\mu\text{m}$  feature that uniquely arises from H<sub>2</sub>O. We used the long-slit FORCAST [9] grism spectrometer (2.4" wide by 180" long) placed on 8 adjacent positions in the region to build tiles, with a reference pointing in Mare Fecunditatis. Nine tiles were observed, divided by their reference, then combined into a spatial-spectral data cube.

Figure 1 shows an example spectrum near Curtius crater. The lunar H<sub>2</sub>O feature is the broad 6.1  $\mu\text{m}$  peak, which is an emissivity excess from an H-O-H bending mode. This is in contrast to the near-infrared 3  $\mu\text{m}$  feature which is a reflectivity dip due to an O-H stretching mode that could arise from H<sub>2</sub>O and OH.



**Figure 1.** (TOP) Spectrum of a single pixel (blue), with continuum fit (orange). (BOTTOM) Emissivity spectrum derived by dividing the observed by continuum fit.

**Distribution of water across the surface:** The 6.1  $\mu\text{m}$  lunar water feature was detected over much of the observed region, but with significant structure. In addition to an overall trend of more water toward earlier lunar time of day, there is a decrease from  $-65^\circ$  latitude to the south pole. Figure 2 shows the sky-plane H<sub>2</sub>O map for the observed region, which spans from Moretus to Manzinus craters on the west and east, and from Curtius to the lunar limb (including the South Pole) from north to south. The H<sub>2</sub>O feature is prominent only in the western side of the field. The eastern part of the region has less water and even an apparent negative feature on the easternmost side. Recalling the reference scheme described above, this means that the eastern side of the observed region has less H<sub>2</sub>O than the Mare Fecunditatis reference, at the time of observation.



**Figure 2.** False-color image showing the distribution of water (blue) in a 3x3' portion of the southern hemisphere including the south pole. The yellow color shows the continuum emission. The water occupies the northern-inner rims of the craters, which are shaded.

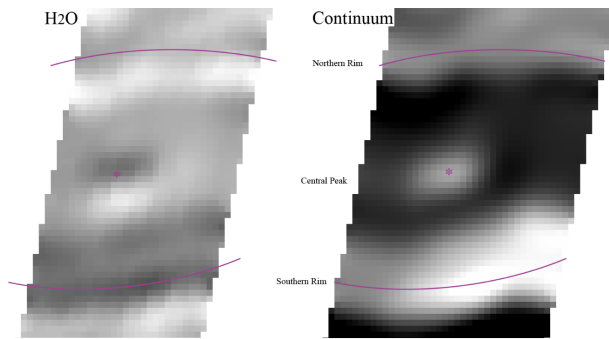


**Figure 3.** An excerpt from Figure 2 centered on Moretus crater. Magenta arcs show the crater rims, which are evident in the continuum image (right). The H<sub>2</sub>O emission (left) is systematically shifted away from the sun (which illuminates the crater from the top of the image).

Figure 3 shows the region of Moretus crater. The H<sub>2</sub>O has a distinct distribution, being systematically on shifted from the hot, sunward surfaces to the cooler, poleward ones. Most notable is the distinct pattern of the central peak. While the continuum image shows a simple brightness feature at the central peak, the H<sub>2</sub>O image has a “dipolar” morphology, with the northern face having a weaker H<sub>2</sub>O feature than the crater floor, and the southern face having significantly more. We were able to confirm this result on one of SOFIA’s last observing flights, where the dipolar pattern again appeared.

Both the northern and southern faces of the Moretus central peak have extensive, steep (60°) slopes, extending vertically to 2.5 km above the crater floor. The base of the central peak has a size comparable to the physical resolution of the data (4.5 km), and the elongated shape is consistent with foreshortening of the crater at -70° latitude. This means that some of the spatial variation in temperature and water abundance is smoothed out by the observing technique. Nonetheless the data reveal a clear excess of H<sub>2</sub>O on the southern face as well as a clear deficit (relative to surroundings) in H<sub>2</sub>O on the northern face of the central peak. The excess emission is likely related to shadowing, as the duration of insolation is much shorter per lunar day on the southern side. The decrease of water on the northern side of the central peak, below the water level at the floor of the crater, indicates that the steep northern slopes lose their water at a significantly higher rate, due to their long exposure to sunlight each lunar day. The steep slopes of the central peak could also lead to different regolith properties and depth, but the strong distinction between water on the north and south sides suggest insolation is a more significant effect in controlling the water distribution.

**Closer to the pole:** On the date of the SOFIA observation, the lunar south pole and a small portion of the far side were visible from Earth. To show the distribution of water closer to the south pole, Fig. 5 shows an orthographic projection. Significant local concentrations of water emission follow the northern rim of Cabeus, the center of Haworth, and the southern rim of Nobile. Compared to the trends seen at higher latitudes, the Cabeus northern rim is consistent with what was seen at Curtius, Moretus, and other craters. These craters all contain permanently shadowed regions and include evidence of water ice, notably Cabeus from the LCROSS impact (18), so the near-polar craters may have larger regions that are amenable to procuring and/or retaining molecular water (33). The molecular water emission closely follows the location of shadows in the LRO image. The strong peak of molecular water on the southern rim of Nobile may be of interest to inform the VIPER rover (28), which is set to explore that region in late 2024.

**Conclusions:** The presence of significant small-scale variations in water content associated with topographic features, with amplitude comparable to the latitude variation, shows that local processes on the lunar surface control the distribution of water as much as an exogenic input. The systematic shift of water distribution away from solar illumination shows that the water has higher abundance just south of the topographic maxima. As the mapped region is in the far southern hemisphere, the shift is consistent with more water in the more-shadowed regions hidden for longer portions of the day by local topographic maxima.

**Acknowledgments:** Based on observations made with the NASA/DLR Stratospheric Observatory for Infrared Astronomy (SOFIA). SOFIA was jointly operated by the Universities Space Research Association (USRA), under NASA contract NNA17BF53C, and the Deutsches SOFIA Institut (DSI) under DLR contract 50 OK 2002 to the University of Stuttgart. Financial support for this work was provided by NASA through award #09\_0171 issued by USRA.

**References:** [1] Pieters, C. M. et al. (2009), *Science* 326, 568. [2] Colaprete, A. P. et al. (2010), *Science* 330, 463. [3] Hendrix, A. R. et al. (2019), *GRL* 46, 2417. [4] Crotts, A. (2011) *Astron. Rev.* 6, 4. [5] Lucey, P. G. et al. (2022) *Geochemistry* 3, 125858. [6] Honniball et al. (2021) *Nature Ast.*, 5, 121; and (2022) *GRL* 49, e97786. [7] Colaprete et al. (2020), *LPI* 51m 2241. [8] Young, E. T. et al. (2012), *Ap. J.* 749, L17. [9] Herter, T. L. et al. (2012) *Ap. J.* 749, L18